Vol 18 No 2, February 2009
1674-1056/2009/18(02)/0636-10

Chinese Physics B

© 2009 Chin. Phys. Soc.
and IOP Publishing Ltd

Study on random and coherence states using a family of CML models

Liu Zhao-Cun(刘兆存)†

Dalian University of Technology, Dalian 116024, China

(Received 22 May 2008; revised manuscript received 24 September 2008)

A family of coupled map lattice (CML) models has been developed to simulate the interaction of convection, diffusion and dispersion in both weakly and strongly coupled cases. With variation of parameters, the models can simulate those systems of convection dominating, diffusion dominating, and dispersion dominating states. Not only coherent and turbulent properties as well as their interrelations, but also the transitional state between any modes with local coupling and global coupling are analysed to demonstrate the essential characteristics of any state. Numerical results show that the models are capable of simulating both layered coupling and stochastic mechanism, and thus can be conveniently used to analyse an initiative and driven coupled system. Results of numerical simulation also lead us to understand whether or not turbulence coherent structure is formed by modulation of wave packet. Finally, the duality of wave and particle characters of turbulence is illustrated in the numerical simulation.

Keywords: CML model, dissipation, dispersion, coherence
PACC: 4660D, 4752, 0565

1. Introduction

The study of large assemblies of chaotic elements that can spontaneously evolve to a state of large scale synchronization and form different patterns is of importance in understanding nonlinear dynamical systems with many degrees of freedom and their potential applications in evolutionary dynamics, fluid dynamics and chemical reaction, etc. The relatively simple coupled map lattice (CML) model – a discrete space and discrete time system of interacting elements whose states vary continuously according to specific functions – is often taken as a convenient tool to study the characteristics of spatiotemporal systems. Starting with the work of Kaneko,[1] spatially extended systems are commonly described using CML models which exhibit a wide variety of complex spatiotemporal behaviours including spatiotemporal chaos, spatiotemporal coherence and various spatiotemporal patterns depending on parameters of CML model.[2−15] A general scenario for the occurrence of turbulence is spatiotemporal intermittency, i.e., a sustained regime characterized by the coexistence of coherent-laminar and disordered-chaotic domains in space and time.[3,4] Recently, there have been many research results obtained not only for discrete dynamical system (hereafter dynamical system) itself but also for dynamical system with turbulence.[2−4] These results have been used to explain other natural phenomena, such as collective cooperative behaviour,[4−6] synchronization, time-delay and phase relation,[7−9] turbulent phenomenon of dynamical system,[10−12] etc. There are also many research results about mathematical properties of dynamical systems. The early results were comprehensively described by Cross and Hohenberg,[13] while recent representative methods and suggestions for future work about synchronization phenomena were reviewed by Acebron *et al.*[14] Some results about patterns can be found in Ref.[15]. All the research activities so far can be summarized as follows: (a) to establish some representative and simple models, and analyse their general properties; and (b) to develop diverse and complicated models to validate the study of the properties so as to draw fundamental laws. The following model corresponding to one-dimensional diffusive mechanism has been extensively used in most of research activities:

$$x_{(n+1)}(i) = (1-\epsilon)f(x_n(i)) + \frac{\epsilon}{2}[f(x_n(i-1)) + f(x_n(i+1))] + p_n(i), \quad (1)$$

where $n = 1, 2, \ldots, T$ is discrete time intervals, $i = 1, 2, 3, \ldots, N$ denotes discrete lattice with periodical spatial boundary, $f(x)$ is a Logistic mapping (or other

†Corresponding author. E-mail: liuzc17@yahoo.com.cn

forms of mapping), and $p_n(i)$ is a local coupling or global coupling. It is important to extend the above model (1) to physical interactions and coupling ways. Some scientists think that turbulence is not only a physical process of the interaction between dissipation and dispersion of turbulent eddies, but also possesses the duality of wave and particle characters, which is closely related to energy inversion. Considering only the turbulence viscosity and dispersion forces in the one-dimensional (1D) case, KdV-Burgers (KdV-B) equation $\frac{\partial u}{\partial t} + u\frac{\partial u}{\partial x} - \gamma\frac{\partial^2 u}{\partial^2 x} + \beta\frac{\partial^3 u}{\partial^3 x} = 0$ is the control equation of turbulence.[16−18] Frisch[19] gave a poor-man's Navier–Stokes equation (Eq.(3.1) in Ref.[19], i.e. $v_{t+1} = 1 - 2v_t^2$) as a CML model to describe the properties of fully developed turbulence. With understanding of the properties of the CML model corresponding to the 1D KdV-B equation,[20] it is useful to investigate the turbulent properties of the CML model using 1D and 2D KdV-B equations, which is beset by randomness, convection, dissipation and dispersion, to illustrate the mechanism of coherence of turbulence qualitatively.

The objective of this paper is to develop a new family of CML models capable of describing interactions of stochastic types of convection, diffusion and dispersion in compound modes of local coupling and global coupling. Numerical results will show that the model is feasible to simulate the coupled functions of various factors and the phenomena in open systems. Many existing models are special cases of the current model.

In the present paper, the new models are developed in section 2. Section 3 presents the simulation results. Structure analysis of the models are given in section 4. Discussions and conclusions are presented in sections 5 and 6, respectively.

2. One-dimensional CML models

We consider the difference form of the following partial differential equation (PDE):

$$\frac{\partial u}{\partial t} - \gamma\frac{\partial^2 u}{\partial^2 x} = 0. \tag{2}$$

Using a forward-in-time and central-in-space difference approximation (FTCS) scheme, one obtains

$$\frac{u_i^{n+1} - u_i^n}{\Delta t} = \gamma\frac{u_{i+1}^n - 2u_i^n + u_{i-1}^n}{(\Delta x)^2}. \tag{3}$$

If $\frac{\epsilon}{2} = \frac{\gamma\Delta t}{\Delta x^2}$, then the above equation can be rewritten as

$$u_i^{n+1} = (1-\epsilon)u_i^n + \frac{\epsilon}{2}(u_{i+1}^n + u_{i-1}^n). \tag{4}$$

With reference to the method and the interpretation of CML model developed by Kaneko,[1] the following model is developed corresponding to PDE (2):

$$\begin{aligned} x_{n+1}(i) =& (1-\epsilon)f(x_n(i)) + \frac{\epsilon}{2}[f(x_n(i+1)) \\ &+ f(x_n(i-1))]. \end{aligned} \tag{5}$$

If other factors, such as feedback in an open system case, are considered by adding another term, $p_n(i)$, the above model becomes model (1) often used by many researchers. The function $f(x)$ is the Logistic mapping or other types of mapping, while the $p_n(i)$ is the local coupling or global coupling. If $p_n(i) = (\epsilon - \epsilon_1)f(x_n(i)) + \frac{\epsilon_1}{N}\sum_{i=1}^{N} f(x_n(i))$, it then becomes the model adopted by Pineda and Cosenza.[21] If $p_n(i) = 0$, it becomes the 2D model adopted by Francisco and Muruganandam.[22] It may reveal a new physical mechanism when extending the above model (1) to include physical interactions and coupling ways.

The equation of KdV–B in 1D case is

$$\frac{\partial u}{\partial t} + u\frac{\partial u}{\partial x} - \gamma\frac{\partial^2 u}{\partial^2 x} + \beta\frac{\partial^3 u}{\partial^3 x} = 0, \tag{6}$$

where $\gamma > 0$, $\gamma\frac{\partial^2 u}{\partial^2 x}$ is often called the dissipative term and $\beta\frac{\partial^3 u}{\partial^3 x}$ the dispersive term. We now consider the difference form of the following PDE:

$$\frac{\partial u}{\partial t} + u\frac{\partial u}{\partial x} - \gamma\frac{\partial^2 u}{\partial^2 x} + \beta\frac{\partial^3 u}{\partial^3 x} = g(u, x, t). \tag{7}$$

Using the control volume method[23] to discretize the above equation, we have

$$\begin{aligned} (1+a_i)u_i^n =& (a_{i+1})u_{i+1}^n + (a_{i-1})u_{i-1}^n \\ &+ u_i^{n-1} + \widetilde{g}(x,t) - \theta[u_{i+2}^{n-1} - 2u_{i+1}^{n-1} \\ &+ 2u_{i-1}^{n-1} - u_{i-2}^{n-1}], \end{aligned} \tag{8}$$

where

$$
\begin{aligned}
&a_{i+1} = \varepsilon_{\rm e} A(|P_{\rm e}|) + [-F'_{\rm e}, 0],\\
&a_{i-1} = \varepsilon_w A(|P_w|) + [F'_w, 0],\\
&a_i = a_{i+1} + a_{i-1} + (F'_{\rm e} - F'_w),\\
&D_{\rm e} = \frac{\gamma_{\rm e}}{\Delta x}, \quad D_w = \frac{\gamma_w}{\Delta x},\\
&F_{\rm e} = 0.5u_{\rm e}, \quad F_w = 0.5u_w,\\
&P_{\rm e} = \frac{F_{\rm e}}{D_{\rm e}}, \quad P_w = \frac{F_w}{D_w},\\
&\varepsilon_{\rm e} = \frac{\gamma_{\rm e}\triangle t}{(\Delta x)^2}, \quad \varepsilon_w = \frac{\gamma_w \Delta t}{(\Delta x)^2},\\
&F'_{\rm e} = \frac{0.5u_{\rm e}\Delta t}{\Delta x}, \quad F'_w = \frac{0.5u_w \Delta t}{\Delta x},\\
&\theta = \frac{\beta \Delta t}{2(\Delta x)^3},\\
&\widetilde{g}(x,t) = g(x,t)\Delta t,\\
&u_{\rm e} = 0.5(u_i + u_{i+1}),\\
&u_w = 0.5(u_i + u_{i-1}).
\end{aligned} \tag{9}
$$

The method by which model (1) and model (5) were developed from Eq.(1) is adopted here. Equation (7) is finally developed to

$$
\begin{aligned}
(1+a_i)u_i^n =&(a_{i+1}+\lambda)u_{i+1}^n + (a_{i-1}-\lambda)u_{i-1}^n\\
&- \theta[f(u_{i+2}^{n-1}) - f(u_{i+1}^{n-1})\\
&+ f(u_{i-1}^{n-1}) - f(u_{i-2}^{n-1})]\\
&+ f(u_i^{n-1}) + \widetilde{g}(x,t),
\end{aligned} \tag{10}
$$

where

$$
\begin{aligned}
\widetilde{g}(x,t) =& g(x,t)\Delta t\\
=& \frac{\chi}{N}\sum_{j=1}^{N} f(u_j^{n-1}), \quad 0 \le \chi \le 1,
\end{aligned} \tag{11}
$$

and $1 \le i \le N$, N=100 is the size of the system (numerical results have shown that there is no essential influence of value of N on the evolution of models; by the way, N may take other numbers), Δx and Δt are spatial step and time interval, respectively, χ is a random variable uniformly distributed within (0,1). Moreover,

$$
A(|P|) = [[0, (1 - 0.1|P|)^5]]. \tag{12}
$$

The $[[a, b]]$ means the larger term of a and b. Other symbols are the same as those given above. The parameter γ takes positive random number in the range of (–1, 1), while β takes random number in the range of (–1, 1), therefore, ϵ is always positive. λ can be positive or negative. Parameters stated above take the same values in each iterative step and take different values in different iterative steps and, finally, become pseudo-random numbers. The function $f(x)$ takes the following Logistic mapping:

$$
\begin{aligned}
&f(x) = 1 - ax^2, \quad a \in [0, 2],\\
&x \in [-1, 1], \quad f(x) \in [-1, 1].
\end{aligned} \tag{13}
$$

The value of entropy can be calculated by using the following equation:

$$
S_{\rm p} = -\sum_{i,j} Q(i,j)\lg Q(i,j). \tag{14}
$$

Here, $Q(i,j)$ is the probability of spatial point u_i in the range of (i,j) . Let

$$
P(n) = \frac{1}{N}\sum_{j=1}^{N}(u_j^n). \tag{15}
$$

The calculation method for Hurst index (hereafter H) can be found in Ref.[24]. Numerical simulation showed that H is a variable affected by sample capacity, data arrange sequence which would be studied in detail in other papers. The grouping arithmetic average of R/S method is adopted in this paper to calculate Hurst index. Compared with known results,[24] the H index can also be used to guarantee correctly demonstrating problems. For convenience, it is called Hurst index, even though it should be correctly called pseudo Hurst index. Boundary conditions are periodic, and initial conditions take random value. Some first 6000 steps are discarded. Many numerical simulations have shown that regardless how many iteration steps are discarded, the final results are independent of iterative times. There is no essential difference in final conclusions obtained from results of 4000 iterative times or 8000 iterative times. The modelling results are given as follows.

Let a of Logistic mapping be 0.99, Δt =1.32 and Δx =5.02, γ take positive random number in the range of (–1, 1), and β take random number in the range of (–1, 1). We have $S_{\rm p}$=0.078. Figure 1 shows relations of $U - I - T$ for the final 100 iterative steps, where T is iterative step. Figure 2 illustrates the relations of $U - T$ for the final 100 iterative steps at I=50. Figure 3 is Hurst index of each lattice I for the last

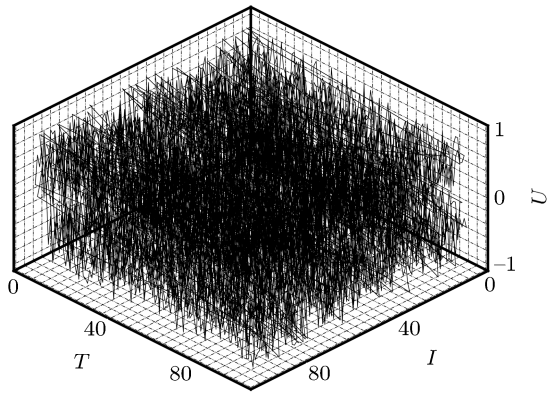


Fig.1. $U - I - T$ diagram.

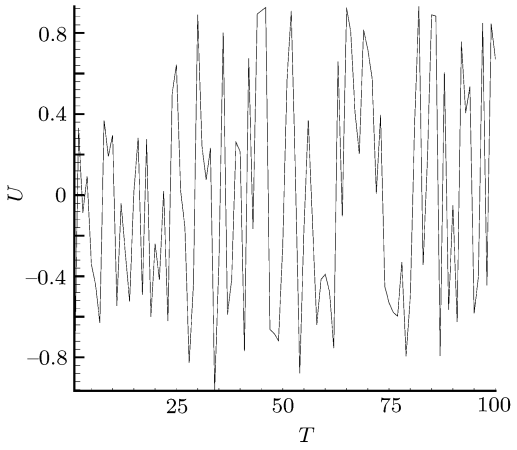


Fig.2. $U - T$ curve.

100 steps, and Fig.4 is phase track of $P(n)$ and $P(n-1)$ (illustrations of following figures are just the same as these). Figure 5 shows the average value

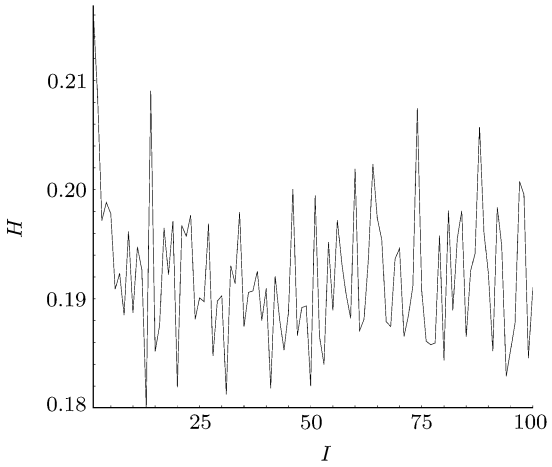


Fig.3. $H - I$ curve.

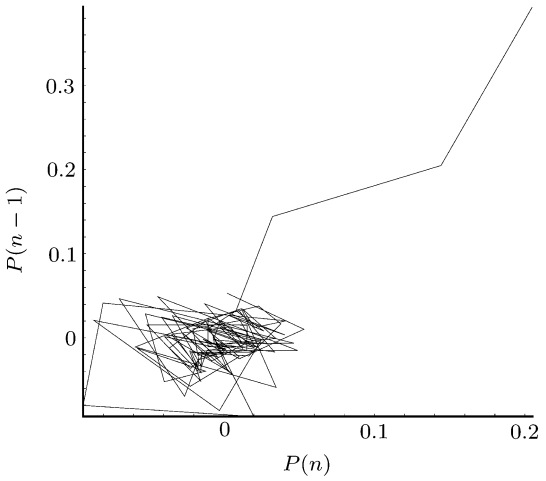


Fig.4. Variation of $P(n-1)$ with $P(n)$.

(mathematical expectation $E(u)$) of each lattice I for the last 100 steps, and Fig.6 depicts variance (standard deviation $D(u)$) of each lattice I for the last 100 steps. If we choose different values for some parameters, for example, a =0.21, Δt =1.32 and Δx =2.38, while keeping other parameters unchanged, then S_{p}=1.09. The shapes of the above figures are changing with essentially the same varying trends. Moreover, if some terms vanish, it becomes the known CML models corresponding to equations $\dfrac{\partial u}{\partial t} = \dfrac{\partial^2 u}{\partial^2 x}$ and $\dfrac{\partial u}{\partial t} + u\dfrac{\partial u}{\partial x} = \dfrac{\partial^2 u}{\partial^2 x}$, numerical results have shown that the models developed in the present paper is consistent with those in Ref.[25] (we do not give these calculated results here).

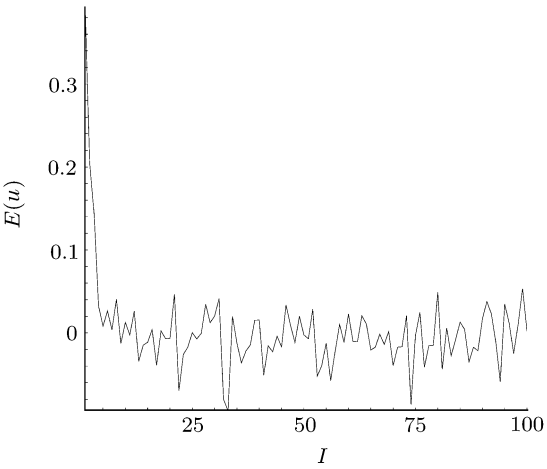


Fig.5. $E(u) - I$ curve.

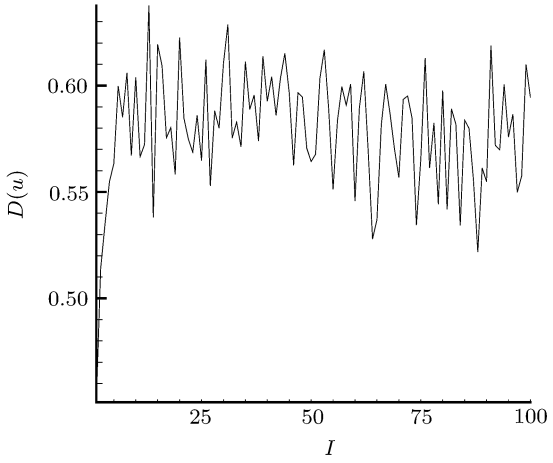


Fig.6. $D(u) - I$ curve.

3. Two-dimensional CML models

In the 2D case, we consider the following PDE:

$$\frac{\partial\left(\dfrac{\partial u}{\partial t}+\tau u\dfrac{\partial u}{\partial x}-\gamma\dfrac{\partial^2 u}{\partial^2 x}+\beta\dfrac{\partial^3 u}{\partial^3 x}\right)}{\partial x}+\alpha\frac{\partial^2 u}{\partial^2 y}$$
$$=h(u,x,t). \tag{16}$$

If the discrete method used above is adopted, then we can obtain the corresponding discrete form as

$$\begin{aligned}
&(1+A_i)u^n_{i+1,j}-A_{i+2}u^n_{i+2,j}\\
&-(1+A_{i-1})u^n_{i-1,j}+A_{i-2}u^n_{i-2,j}\\
&+2B_j u^n_{i,j+1}+2B_j u^n_{i,j-1}-4B_j u^n_{i,j}\\
=&h'(u,x,t)+[u^{n-1}_{i+1,j}-u^{n-1}_{i-1,j}]\\
&-\lambda[u^{n-1}_{i+3,j}-2u^{n-1}_{i+2,j}-u^{n-1}_{i+1,j}+4u^{n-1}_{i,j}\\
&-u^{n-1}_{i-1,j}-2u^{n-1}_{i-2,j}+u^{n-1}_{i-3,j}],
\end{aligned} \tag{17}$$

where

$$B=\frac{\alpha}{\Delta x}\Delta t(\Delta y)^2,$$

$$h'(u,x,t)=2h(u,x,t)\Delta x\Delta t,$$

Δx and Δy are spatial steps in x and y directions respectively, α is coefficient ($0<\alpha<1$), and other symbols are the same as those given above. The following model is developed with the identical approach as before:

$$\begin{aligned}
&-A_{i+2,j}u^n_{i+2,j}+(1+A^+_{i+1,j})u^n_{i+1,j}-(1+A^-_{i-1,j})u^n_{i-1,j}+A^-_{i-2,j}u^n_{i-2,j}\\
&+2B_{i,j+1}u^n_{i,j+1}+2B_{i,j-1}u^n_{i,j-1}-[4B_{i,j}+A^+_{i,j}-A^-_{i,j}]u^n_{i,j}\\
=&[R(u^{n-1}_{i+1,j})-R(u^{n-1}_{i-1,j})]-\lambda_{i-1,j}[R(u^{n-1}_{i+1,j})-2R(u^{n-1}_{i,j})+2R(u^{n-1}_{i-2,j})-R(u^{n-1}_{i-3,j})]\\
&-\lambda_{i+1,j}[R(u^{n-1}_{i+3,j})-2R(u^{n-1}_{i+2,j})+2R(u^{n-1}_{i,j})-R(u^{n-1}_{i-1,j})]\\
&+\xi_1(n)\left(R\left(\frac{1}{NI\times NJ}\sum_{i=1}^{NI}\sum_{j=1}^{NJ}u^{n-1}_{i,j}\right)\right)\cos\left(\frac{1}{NI\times NJ}\sum_{i=1}^{NI}\sum_{j=1}^{NJ}u^{n-1}_{i,j}\right)\\
&+\xi_2(n)(u^{n-1}_{i,j})\cos(u^{n-1}_{i,j})+0.25\times\sum_{-2\le ij\le 2,ij\neq 0}\xi_{ij}(n)R(u^{n-1}_{i,j}-u^{n-1}_{i-ij,j})\times\cos(u^{n-1}_{i,j}-u^{n-1}_{i-ij,j}),
\end{aligned} \tag{18}$$

where $1\le i\le NI$, $1\le j\le NJ$, and NI and NJ are system sizes in x and y directions, respectively. Here, $NI=NJ=100$. Numerical results have shown that there is no essential influence of NI and NJ on the evolution of models. $\xi_1(n)$, $\xi_2(n)$ and $\xi_{ij}(n)$ (where $-2\le ij\le 2$ and $ij\neq 0$, ij are integers) are random numbers uniformly distributed within (0,1). Moreover, $A^+_{i+1,j}$, $A^+_{i+2,j}$ and $A^+_{i,j}$ are calculated values provided that $(i+1,\ j)$ is a centre point just as in 1D case above. So are $A^-_{i-1,j}$, $A^-_{i-2,j}$ and $A^-_{i,j}$ provided that $(i-1,\ j)$ is a centre point (see Ref.[25]). The function $R(x)$ is similar to the Tent Map, i.e.

$$R(x)=\begin{cases}
-2-2x, & -1\le x\le -0.5, & \text{(19a)}\\
2x, & -0.5<x\le 0.5, x\in[-1,1], R(x)\in[-1,1], & \text{(19b)}\\
2-2x, & 0.5<x\le 1-x. & \text{(19c)}
\end{cases}$$

The entropy could be calculated by using Eq.(14). The boundary conditions are periodic, and the initial conditions are random. The modelling results partially correspond well with the known results.[26,27] Let Δt =0.74, Δx =0.87, Δy =1.61, a=0.40, α =0.65, β =0.12, γ =0.73 and τ =1.00, then S_p=1.06 is obtained while the other parameters keep the same as those in 1D case. Figure 7 shows the relation of U-I-J for the final 100 iterative steps. Figure 8 illustrates

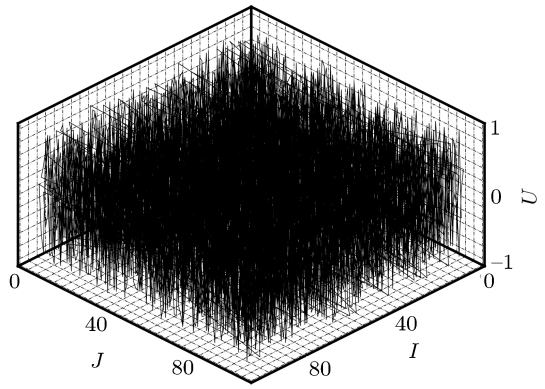


Fig.7. The $U - I - J$ diagram.

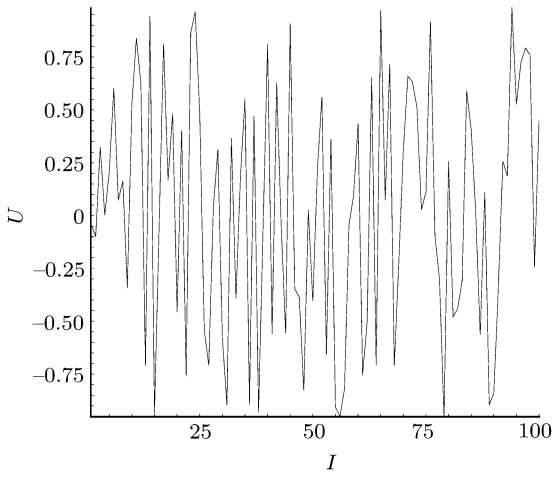


Fig.8. Variation of U with I.

the relations of $U - I$ for the final 100 iterative steps and Fig.9 illustrates the relations of $U - J$ for the final 100 iterative steps, in Figs.(8) and (9), J=50 and T=50. The Hurst index of each lattice in J direction, i.e. the direction parallel to J plane in Fig.8, is shown in Fig.10. Figure 11 depicts the Hurst index of each lattice in I direction. The mathematical expectation and the standard deviation of each lattice in J direction, i.e. the direction parallel to J plane shown in Fig.8, are shown in Figs.12 and 13 respectively. The numerical modelling results have shown that the cases in I direction are similar to those shown in J direction. Let some parameters

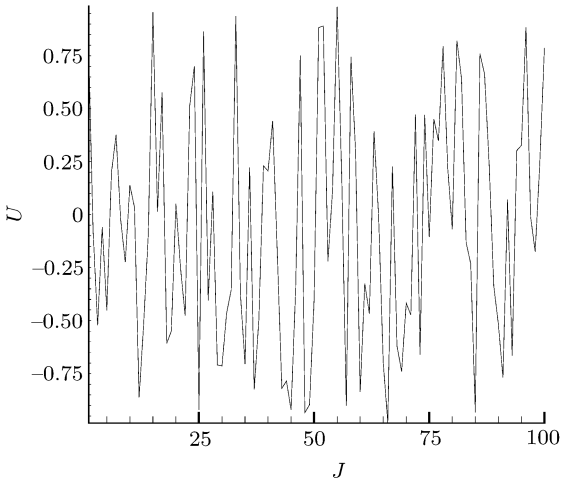


Fig.9. Variation of U with J.

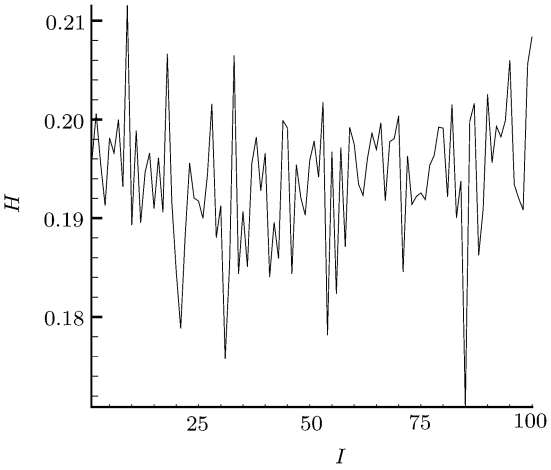


Fig.10. Variation of H with I.

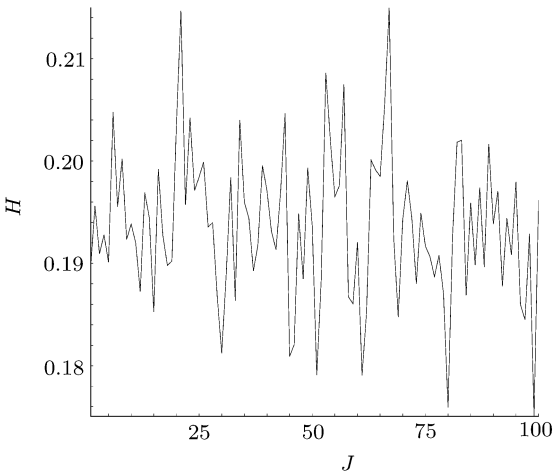


Fig.11. Variation of H with J.

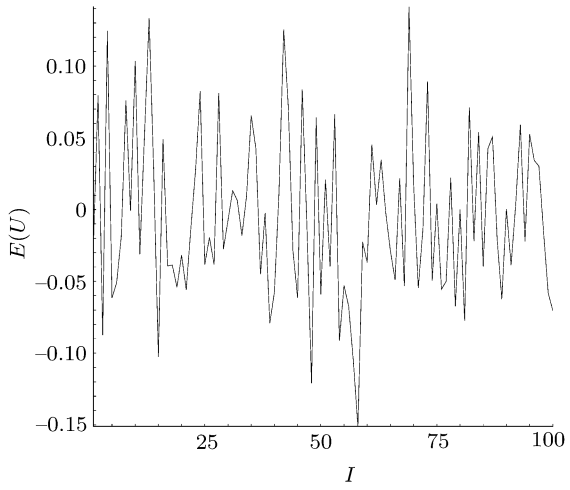


Fig.12. Variation of $E(u)$ with I.

have different values, e.g., Δt =0.14, Δx = 2.35, Δy =1.31, a=0.12, α =0.96, β =0.51, γ =0.17, and τ =0.52, and then S_p=1.06 is obtained while the other parameters keep the same as those in 1D case. As a result, the shapes of the above figures (Figs.7–13) would change even though the changing trends are essentially identical. Let some terms vanish, then the numerical results of the known CML models corresponding to equations of $\dfrac{\partial u}{\partial t} + u\dfrac{\partial u}{\partial x} = \dfrac{\partial^2 u}{\partial^2 x}$ and $\dfrac{\partial u}{\partial t} + u\dfrac{\partial u}{\partial x} - \gamma\dfrac{\partial^2 u}{\partial^2 x} + \beta\dfrac{\partial^3 u}{\partial^3 x} = 0$, show that the models developed here have results consistent well with those in Ref.[25]. After final iteration is finished, the variables could be subject to the following transform procedure

$$u_{i,j} = u_{i,j0} + u_{i,js}, \tag{20}$$

where $u_{i,js}$ is a random variable following the Gaussian normal distribution law, of which the mathematical expectation and deviation are shown as follows:

$$E(u_{i,js}) = \lambda_{\mathrm{ex}}\left(\frac{1}{NI \times NJ}\sum_{i=1}^{NI}\sum_{j0=1}^{NJ} u_{i,j0}\right), \tag{21}$$

$$D(u_{i,js}) = \lambda_{dx}\sqrt{\frac{1}{NI \times NJ - 1}\sum_{i=1}^{NI}\sum_{j0=1}^{NJ}(u_{i,j0} - E(u_{i,j0}))^2}. \tag{22}$$

Let λ_{ex}=0.7, λ_{dx}=0.1. The values of random variable could be obtained with the Monte-Carlo method, while the other parameters are the same as those in Fig.7. Figure 14 shows the relation of $U-I-J$, where the entropy S_{p} is equal to 0.0. The numerical results show that other calculated results are similar to those in Figs.8–13.

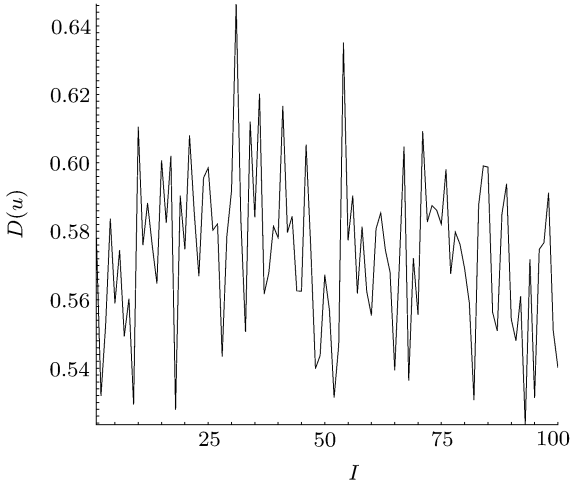


Fig.13. Variation of $D(u)$ with I.

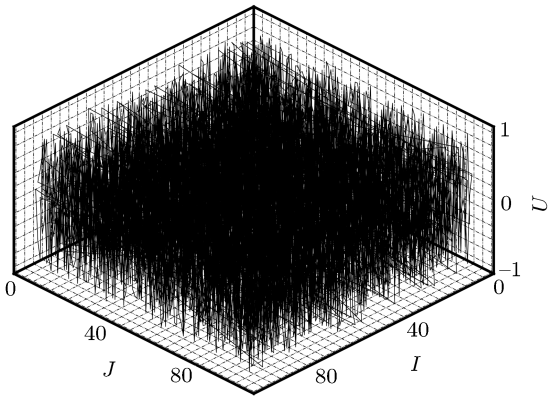


Fig.14. The $U-I-J$ diagram.

In 2D case, the following PDE is considered

$$\frac{\partial\left(\dfrac{\partial u}{\partial t} + g(x,y,t,u)\times u\dfrac{\partial u}{\partial x} - \gamma(x,y,t,u)\dfrac{\partial^2 u}{\partial^2 x} + \beta(x,y,t,u)\dfrac{\partial^3 u}{\partial^3 x}\right)}{\partial x} + \alpha(x,y,t,u)\frac{\partial^2 u}{\partial^2 y} = h(u,x,y,t). \tag{23}$$

If the discrete method mentioned above is adopted, then the discrete form of the equation could be obtained

$$\begin{aligned}&(1+A_i)u^n_{i+1,j}-A_{i+2}u^n_{i+2,j}-(1+A_{i-1})u^n_{i-1,j}+A_{i-2}u^n_{i-2,j}+2B_ju^n_{i,j+1}+2B_ju^n_{i,j-1}-4B_ju^n_{i,j}\\ =&h'(u,x,t)+[u^{n-1}_{i+1,j}-u^{n-1}_{i-1,j}]-\lambda[u^{n-1}_{i+3,j}-2u^{n-1}_{i+2,j}-u^{n-1}_{i+1,j}+4u^{n-1}_{i,j}-u^{n-1}_{i-1,j}-2u^{n-1}_{i-2,j}+u^{n-1}_{i-3,j}],\end{aligned}\tag{24}$$

where $B_{i,j}=\dfrac{\alpha_{i,j}\Delta x\Delta t}{(\Delta y)^2}$, $h'(u,x,t)=2h(u,x,t)\Delta x\Delta t$, Δx and Δy are spatial steps in x and y directions respectively, $\alpha_{i,j}$ is the random coefficient ($0<\alpha_{i,j}<1$). Then the following model could be developed

$$\begin{aligned}&-A_{i+2,j}u^n_{i+2,j}+(1+A^+_{i+1,j})u^n_{i+1,j}-(1+A^-_{i-1,j})u^n_{i-1,j}+A^-_{i-2,j}u^n_{i-2,j}\\ &+2B_{i,j+1}u^n_{i,j+1}+2B_{i,j-1}u^n_{i,j-1}-[4B_{i,j}+A^+_{i,j}-A^-_{i,j}]u^n_{i,j}\\ =&[R(u^{n-1}_{i+1,j})-R(u^{n-1}_{i-1,j})]-\lambda_{i-1,j}[R(u^{n-1}_{i+1,j})-2R(u^{n-1}_{i,j})+2R(u^{n-1}_{i-2,j})-R(u^{n-1}_{i-3,j})]\\ &-\lambda_{i+1,j}[R(u^{n-1}_{i+3,j})-2R(u^{n-1}_{i+2,j})+2R(u^{n-1}_{i,j})-R(u^{n-1}_{i-1,j})]\\ &+\xi_1(n)\left(R\left(\frac{1}{NI\times NJ}\sum_{i=1}^{NI}\sum_{j=1}^{NJ}u^{n-1}_{i,j}\right)\right)\cos\left(\frac{1}{NI\times NJ}\sum_{i=1}^{NI}\sum_{j=1}^{NJ}u^{n-1}_{i,j}\right)+\xi_2(n)(u^{n-1}_{i,j})\cos(u^{n-1}_{i,j})\\ &+0.25\times\sum_{-2\le ij\le 2,ij\ne 0}\xi_{ij}(n)R(u^{n-1}_{i,j}-u^{n-1}_{i-ij,j})\times\cos(u^{n-1}_{i,j}-u^{n-1}_{i-ij,j}),\end{aligned}\tag{25}$$

where $1\le i\le NI$, $1\le j\le NJ$. The $\xi_1(n)$, $\xi_2(n)$ and $\xi_{ij}(n)$ are random variables uniformly distributed within (0,1) respectively. Moreover,

$$\begin{aligned}B_{i,j}&=\frac{\alpha_{i,j}\Delta x\Delta t}{\Delta y^2},\\ B_{i,j-1}&=\frac{\alpha_{i,j-1}\Delta x\Delta t}{\Delta y^2},\\ B_{i,j+1}&=\frac{\alpha_{i,j+1}\Delta x\Delta t}{\Delta y^2},\\ \lambda_{i-1,j}&=\frac{\beta_{i-1,j}\Delta t}{2\Delta x^3},\\ \lambda_{i+1,j}&=\frac{\beta_{i+1,j}\Delta t}{2\Delta x^3},\end{aligned}\tag{26}$$

and $A^+_{i+1,j}$, $A^+_{i+2,j}$, $A^+_{i,j}$, $A^-_{i-1,j}$, $A^-_{i-2,j}$, $A^-_{i,j}$ could be calculated by the method mentioned above.

The numerical results show that the evolutional trends of models (25) and (18) are identical, except that the model (25) shows more randomness under the same initial condition and the boundary condition. However, both of them illustrate the identical evolutional mechanism though some measured parameters are different. For example, if let Δt =0.14, Δx =2.35, Δy =1.31, a=0.12, let $\alpha(x,y,t,u)$ and $\gamma(x,y,t,u)$ take the random numbers in the range of [0, 1], let $\beta(x,y,t,u)$ and $g(x,y,t,u)$ take random numbers in the range of [–1, 1], and let other parameters keep the same values as in 1D case, then $S_{\rm p}$=21.60 could be obtained consequently.

4. Model structure analysis

Results of the numerical simulation show that the general tendencies of the models are that the increasing value of parameter a makes the system pattern become chaotic, and the variation of parameter β makes the system pattern changed. The convective mechanism has much influence on the properties and the patterns of system. Variation of the size of the spatial steps and time interval essentially changes the relative importance and ratio among the convective mechanism, the diffusive mechanism and the dispersive mechanism.

The parameter a plays an important role in the system pattern. The specific form of nonlinear function has no more influence on the final whole pattern instead of the local system pattern. Increasing value of parameter γ makes the system pattern become more ordered, and the increase of the convective factor makes the pattern of the system become more sensitive to disturbance. The cooperation of dispersion and dissipation could change the final form of the system pattern. The values of the parameters, such as $S_{\rm p}$ and Hurst index, are not sensitive to what the specific forms of the global coupling and/or the local coupling are, while the specific forms of the global coupling and the local coupling have much effect on the final system pattern. No matter how parameters vary, the local pattern and the whole pattern of the system

show the phenomenon of holograph in a relative large specific zone, just like the pattern on a tiger body.

Transform the function of $f(x)$ and $R(x)$, or let $f(x)$ and/or $R(x)$ take other forms, for example, $\Theta(x)$

$$\Theta(x) = 2\left(\frac{\mathrm{e}+1}{\mathrm{e}}\right)^2\left[(1-\varkappa)\frac{\mathrm{e}^x}{\mathrm{e}^x+1}+\varkappa\frac{\mathrm{e}^x}{(\mathrm{e}^x+1)^2}\right] - \frac{\mathrm{e}+2}{\mathrm{e}}, \tag{27}$$

where $\varkappa \in [0,1]$, $e \approx 2.71828...$, and $x \in [-1,1]$. It is easy to know that $\Theta(x) \in [-1,1]$. Then the shapes of the above figures are changed even though the evolutional laws are identical in essence: the appearance characters of these figures shows chaotic. Symmetry and self-similarity form the dual properties, including both of the order and randomness: on one hand, the evolution is very sensitive to the initial condition and highly instable; on the other hand, the final results of evolution manifest the entire stability to some extent, which forms the particular spatiotemporal pattern. Randomness and determination coexist in these evolutional processes.

An important phenomenon of nonlinear spatiotemporal system is the spatiotemporal resonance which results from the stochastic resonance under certain circumstance. Noise plays an important role in the collective behaviour of nonlinear spatiotemporal system: on one hand, it could do harm to order; on the other hand, it could evoke phase transition to produce ordered power from out-of-order energy, from which results the stochastic resonance or the interference resonance to bring scale competition to form the complicated spatiotemporal pattern. If under different initial condition, different boundary condition, different feedback, or different coupled form were adopted, the models developed in this study would appear the similar patterns in essence, though the pattern in the specific spatiotemporal point or zone might be different and might be very sensitive to initial and boundary conditions. Generally, the equation of CML models determines the form of pattern. The initial condition, the boundary condition, the feedback form and the coupled form determine the pattern's spatiotemporal distribution, the coupled intensity and the coupled form of physical factors in equation choose which evolutional stage of pattern should be.

On the whole, the spatiotemporal patterns of different evolution stages are the dynamic coexistence of the ordered structure and the stochastic structure. The ordered structure and the stochastic structure could mutually transform and always interweave together. So the spatiotemporal pattern corresponding to the KdV-B equation should be a deterministic evolutional result with a stochastic evolutional process.

5. Discussion

The following symbols are adopted:

$$\nabla \equiv \boldsymbol{i}\frac{\partial}{\partial x}+\boldsymbol{j}\frac{\partial}{\partial y}+\boldsymbol{k}\frac{\partial}{\partial z}, \tag{28}$$

$$\Xi \equiv \boldsymbol{i}\frac{\partial^2}{\partial x^2}+\boldsymbol{j}\frac{\partial^2}{\partial y^2}+\boldsymbol{k}\frac{\partial^2}{\partial z^2}, \tag{29}$$

where, $\boldsymbol{i}$, $\boldsymbol{j}$ and $\boldsymbol{k}$ are unit vectors of the Cartesian coordinate system; the symbol $\equiv$ means being defined as. Some scholars prefer that the Reynolds Average Equation of the impressible turbulent flow in the inertial system should be given as follows:

$$\frac{\partial \boldsymbol{u}}{\partial t}+(\boldsymbol{u}\cdot\nabla)\boldsymbol{u} = \boldsymbol{f}-\frac{1}{\rho}\nabla p+\vartheta\nabla^2\boldsymbol{u}-\delta\nabla\cdot\Xi\boldsymbol{u}, \tag{30}$$

$$\frac{\partial \rho}{\partial t}+\nabla\cdot(\rho\boldsymbol{u})=0, \tag{31}$$

where, $\boldsymbol{u}$ represents the velocity, ρ the density, p the pressure, $\boldsymbol{f}$ the unit mass force, ϑ the turbulent viscosity, δ the turbulent dispersive coefficient, and t the time. The Coriolis factor is not considered in the above equations.

Some scholars, e.g. Lin[28] pointed out that turbulence possesses the duality of wave and particle. Others attempted to study turbulence from different approaches, such as electromagnetism,[29] dynamical quantum chaos,[30] relative dispersion,[31] field theory,[32] scaling,[33] etc. These studies present a sketch picture of the duality of wave and particle as follows: 1) The wave character of turbulence can be regarded as that, though the evolutional process of turbulence is random, the patterns formed at each evolutional stage is deterministic, the interactions of which form the wave picture. 2) The particle character of turbulence could be regarded as that, for micro-cluster of the fluid flow, even though in the microscopic scale, their movement governing equation is Navier–Stokes equation. In the long time scale, the turbulent dispersive coefficient δ is equal to 0. However, the turbulent dispersive coefficient is an index to measure the interactions among eddies, and only exists in the turbulent evolutional process, just like the eddy viscosity.

By the way, if there are some kinds of scalings, the scaling corresponding to the limit state of a system is not always the limit of scaling corresponding to a system.

6. Conclusions

Numerical results have shown that the models developed in this study are capable of simulating the physical phenomena, such as convection, diffusion and dispersion, and feasible to simulate both the layered coupling and the stochastic mechanism, with local coupling and global coupling, in both weakly and strongly coupled cases. Many existing models are their special cases.

The merit of the overall state and local coupling of the model is closely related to whether they have a linear or nonlinear form, but not their specific forms. However, the local properties of the model are connected closely with concrete function of the nonlinear mapping $f(x)$. Therefore, the specific form of the model is a local function of spatial points and phases of the evolutionary process.

From the analysis of the simulated results based on the present model, we believe that the turbulence coherent structure is a result of wave packet modulation. It is a random evolutionary process with a deterministic outcome. Resonance mechanism plays an important role in the formation of the coherent structure.

Finally, the duality of wave and particle characteristics of turbulence is schematically illustrated with the simulated results.

Acknowledgements

The author wishes to express his sincere appreciation and gratitude to professors, Gao Ge, Xu Xiangzhou, for their valuable helps and directions during the preparation of the manuscript. His special appreciation is to professor Yan Yong, who kindly permitted him to include some of his results in this paper.

References

[1] Kaneko K 1989 *Physica* D **34** 1
[2] Jensen M H 1989 *Phys. Rev. Lett.* **62** 1361
[3] Zheng Z G 2004 *Spatiotemporal Dynamics and Collective Behaviors in Coupled Nonlinear System* (Beijing: High Education Press) (in Chinese) p152–185
[4] Bohr T, Jensen M H, Paladin G and Vulpiani A 1998 *Dynamical Systems Approach to Turbulence* (Cambridge: Cambridge University Press) p21–47
[5] Pikovsky A S and Kurths J 1994 *Phys. Rev. Lett.* **72** 1644
[6] De Monte S, d'Ovidio F and Mosekilde E 2003 *Phys. Rev. Lett.* **90** 054102
[7] Huber D and Tsimring L S 2003 *Phys. Rev. Lett.* **91** 260601
[8] Nekorkin V I, Kazantsev V B and Velarde M G 2001 *Physica* D **151** 1
[9] Rosenblum M G and Pikovsky A S 2004 *Phys. Rev. Lett.* **92** 114102
[10] Masoller C and Marti A C 2005 *Phys. Rev. Lett.* **94** 134102
[11] Guan S G, Lai C H and Wei G W 2003 *Comput. Phys. Commun.* **155** 77
[12] Aringazin A K 2004 *Phys. Rev.* E **70** 036301
[13] Cross M C and Hohenberg P C 1993 *Rev. Mod. Phys.* **65** 851
[14] Acebron J A, Bonilla L L, Perez C J, Ritort F and Spigler R 2005 *Rev. Mod. Phys.* **77** 137
[15] Gollub J P and Langer J S 1999 *Rev. Mod. Phys.* **71** 5396
[16] Gao G 1985 *Science in China* (Series A) **18** 616
[17] Liu S D and Liu S K 1992 *Science in China* (Series A) **35** 576
[18] Liu S K and Liu S D 1998 *Progress in Nature Science* **8** 629
[19] Frisch U 1995 *Turbulence* (Cambridge: Cambridge University Press) p27–39, p120–159
[20] Liu Z C 2009 *Applied Mathematics and Mechanics* English edition (to appear)
[21] Pineda M and Cosenza M G 2005 *Phys. Rev.* E **71** 057201
[22] Francisco G and Muruganandam P 2003 *Phys. Rev.* E **67** 066204
[23] Randall J L 2002 *Finite Volume Method for Hyperbolic Problems* (Cambridge: Cambridge University Press) p64–84
[24] Liu B Z and Peng J H 2004 *Nonlinear Dynamics* (Beijing: High Education Publishing House) (in Chinese) p317–343
[25] Liu Z C 1998 *Applied Mathematics and Mechanics-English Edition* **19** 881
[26] Fan E G, Zhang J and Benny Y C 2001 *Phys. Lett.* A **29** 376
[27] Ilison O and Salupere A 2005 *Chaos, Solitons and Fractals* **26** 453
[28] Lin C C 1983 *Galaxies, Turbulence and Plasmas* (Beijing: Science Press)
[29] Marnanis H 1998 *Physics of Fluids* **10** 1428
[30] Chiueh T 1998 *Phys. Rev.* E **57** 4150
[31] Boffetta1 G and Sokolov I M 2002 *Phys. Rev. Lett.* **88** 094501
[32] Falkovich G, Gawedzki K and Vergassola M 2001 *Rev. Mod. Phys.* **73** 913
[33] Mazzino A, Ginanneschi P M and Musacchio S 2007 *Phys. Rev. Lett.* **99** 144502